Separation and Purification Technology 389 (2026) 136720

Contents lists available at ScienceDirect

Separation and Purification Technology

journal homepage: www.elsevier.com/locate/seppur

Methodology for the characterization of pleated filter media in a pulse-jet-cleaned test-rig in accordance to DIN ISO 11057

Jakob Paul Knisley *, Jörg Meyer, Achim Dittler

Karlsruhe Institute of Technology, Institute of Mechanical Process Engineering and Mechanics, Straße am Forum 8, Karlsruhe, 76131, Germany

ARTICLE INFO

Communicated by V. Tarabara

Keywords:
Surface filtration
Pleated filter medium
Filter medium characterization
Lab testing

ABSTRACT

The testing, characterization and evaluation of cleanable filter media for gas-cleaning applications are standardized in different standards and VDI guidelines. These procedures characterize flat filter media coupons and rely on specific test setups, methodology and experimental parameters such as the tank pressure for regeneration and filter media face velocity. However, if the geometry of the filter media deviates from the standardized flat coupon, characterization cannot be conducted in the test rig according to these standards. A common modification is pleating/folding the filter media, which allows for an increasing filter media surface area in a smaller installation space. Typically, pleatable filter media are evaluated using flat filter media coupons, with the results subsequently being applied to characterize pleated filter media. Direct characterization of pleated filter media in the pulse-jet-cleaned test-rig can prevent inaccurate conclusions transferred from flat to pleated geometries. To address this limitation, a novel filter holder was developed to enable the direct testing of pleated filter media in a standardized, pulse-jet-cleaned test-rig with harmonized experimental parameters for both media geometries. This allows the same experimental parameters and regeneration efficiency. The operating behavior was evaluated based on cycle time and residual differential pressure. The results show differences between the flat and pleated geometry under identical test conditions. These findings highlight the need for direct characterization of pleated filter media to accurately determine their performance.

1. Introduction

Surface filtration has a long-standing history in applications aimed at separating particles from dust-laden gas streams. After an initial depth filtration stage, during which particles are primarily collected on the fibers within the filter medium, a dust cake forms on the surface of the filter medium. Particle separation within the dust cake, along with the continued accumulation of further particles on the upstream side of the dust cake, results in a high collection efficiency [1]. This enables the reduction of emission levels or the virtually complete recovery of particles from the gas stream [1,2].

Surface filters are commonly operated in cycles, wherein each cycle consists of a filtration period followed by the regeneration of the filter medium. Regeneration is necessary to reduce the differential pressure due to increasing flow resistance of the growing dust cake during filtration. A widespread method for online regeneration is the short-term use of pressurized air directed against the normal flow of filtering gas (pulse-jet) [3]. During stable operation the differential pressure increases due to a progressive thickening of the dust cake on the filter medium and drops to a repeatable low level after each regeneration, resulting in longer filtration periods between regenerations. A thicker dust cake and the deposition of particles inside the fibers of the filter medium result in more efficient particle separation from the gas stream and a decrease in emitted particle size after the filter [4,5]. Consequently, this leads to low emission levels on the clean gas side [4]. However, reducing the differential pressure through regeneration at sufficiently short intervals is essential for maintaining an economical and stable filter operation [6]. Online regeneration of the filter results in a short-term increase in particle concentration on the clean gas side due to particle penetration through the filter medium after the dust cake is removed [7]. This trade-off between longer filtration cycles (which lead to lower emissions, but higher energy consumption by the fan) and shorter cycles (which reduce energy consumption by the fan, but increase emissions) must be carefully considered [8].

One type of surface filters are pleated filter elements, such as pleated filter cartridges or flat pleated panels. Pleating the filter media allows an increase in filtration surface area compared to a flat filter element if both are implemented in the same installation space [9–11]. An important factor in evaluating pleated filter media is the pleat ratio α or

* Corresponding author.
E-mail address: jakob.knisley@kit.edu (J.P. Knisley).

https://doi.org/10.1016/j.seppur.2025.136720
Received 23 October 2025; Received in revised form 30 December 2025; Accepted 30 December 2025
Available online 2 January 2026

pleat count, both of which quantify the degree of pleating. The pleat ratio is defined as the ratio of pleat height to pleat width, while the pleat count describes the number of pleats across the width of the filter element [9,11,12]. The pleat ratio impacts the differential pressure, regeneration efficiency, dust loading characteristic of the filter media, and the effective filtration area. Furthermore, pleating can affect the emission behavior.

Filter media used in pleated elements are generally tested as a flat filter medium coupon, following standards or guidelines, such as DIN ISO 11057 [13] or VDI 3926 [14]. These guidelines evaluate cleanable filter media for surface filtration in a pulse-jet-cleaned test-rig. The assessment is mainly based on the development of residual differential pressure and on the duration of the filtration cycles. Particle emission is measured gravimetrically. The findings from testing the flat filter medium coupon can only partially be transferred to the pleated geometry of the same filter medium. This is due to effects such as the change in medium geometry or in medium properties as a consequence of pleating.

During the pleating process the filter media undergoes mechanical stress, which can alter the local medium thickness and medium permeability (mainly at the tip and the bottom), thereby altering the flow behavior [15]. Pleated filter elements often exhibit shorter cycle times compared to flat elements, primarily attributed to incomplete dust cake detachment during regeneration [16]. Poor regeneration can be attributed to several factors, such as the lack of medium movement during regeneration or the fact, that the dust cake is lodged in the bottom of the pleat [17]. The understanding of the regeneration behavior, such as the maximum peak pressure after the regeneration is triggered or the distribution of the peak pressure across the filter element has been the subject of many studies in the past [18–20], highlighting the arising challenges from altering the filter medium geometry from flat to pleated.

Comparisons between flat and pleated geometries of filter media have been conducted in the past for different size scales. Kim et al. [21] compared a pleated filter cartridge with a cylindrical filter bag, showing that under the same experimental conditions the pleated filter cartridge displayed shorter cycle times, mainly due to the loss in filtration area over time. Li et al. [12] compared a flat filter medium with different pleated geometries and also observed the decrease in cycle time for the pleated geometry compared to the flat medium geometry. Similarly, Teng et al. [10,22] investigated the influence of filter geometry in pleated panel filters, comparing flat and pleated setups while adjusting experimental parameters to maintain identical face velocity and raw-gas concentration. Their results showed varying rates of differential pressure increase for pleated media compared to flat media during dust loading, again emphasizing the influence of geometry on key operational parameters.

Despite numerous studies investigating pleated filter elements, differences in regeneration and operating behavior compared to flat filter elements remain. The most relevant differences concern the development of the residual differential pressure and the cycle time for different geometries. Previous research often lacked harmonized experimental parameters, such as regeneration intensity for different dimensioned filter elements or long-term evaluation of the aged filter media, making the isolation of the influence of geometry on the operating behavior difficult. This study addresses this gap by providing a standardized, directly comparable evaluation of flat and pleated filter media under the same experimental conditions. Furthermore, directly evaluating both geometries under standardized conditions and the same procedure enables an assessment of the transferability of flat media coupon tests of pleatable filter media to the pleated filter media.

To achieve this, pleated filter media with a pleat ratio of two were implemented in a pulse-jet-cleaned test rig based on the DIN ISO 11057 standard to directly characterize pleated filter media. This included the use of a novel filter holder to implement the pleated filter media into the existing test-rig geometry. In addition, a comparative analysis was conducted between a flat medium coupon and one pleated configuration of the same filter medium to evaluate differences in filtration behavior due to a differing geometry. To enable comparison, the experimental parameters for both geometries have to be adapted to ensure identical operating conditions at the media face. Resulting differences in operating behavior for the different media geometries can thus be attributed to the influence of different filter media geometry.

2. Experimental setup, methodology and materials

2.1. Filter media test-rig and filter media implementation

2.1.1. Pulse-jet-cleaned filter media test-rig

The experiments were conducted in a pulse-jet-cleaned test-rig based on DIN ISO 11057, illustrated schematically in Fig. 1. Test dust is fed into the raw gas duct by a dust feeder and the raw gas concentration is continuously monitored using an extinction measurement. The aerosol is partially sucked through the filter medium in a cross-flow from the raw gas side to the clean gas side. The rest of the aerosol is sucked through the raw gas filter and the cleaned air is released as excess air. The regeneration unit consists of a blowpipe, a pressure tank, an electromagnetic cleaning valve, a pressure regulation valve and a connection to the pressurized air line. After the filter regeneration is triggered, the electromagnetic valve opens and releases a pulse-jet directed towards the filter medium through the blow pipe a nozzle with a diameter of $3 \cdot 10^{-3}$ m. The dislodged dust after regeneration is collected in the dust hopper.

Unlike the standard (DIN ISO 11057) the particle emission is not measured gravimetrically, but with an optical particle counter (OPC). The measurement principal of the Promo® 2000 with a Welas® 2300 sensor by the manufacturer Palas® is based on the optical light scattering of single particles. This OPC offers a time and size resolved number concentration as an output. The measurement range of the sensor was set to 0,2–10 µm to better depict the size range of the most penetrating particle size (MPPS) of surface filters, which lies between 0,3–1 µm [7]. The emission measurement in this study was mainly used for monitoring the clean gas emissions.

2.1.2. Filter medium

The filter medium used to characterize both the flat and pleated geometry in the test-rig consisted of thermally bonded PES fibers with an ePTFE membrane on the upstream side. The medium has a thickness of $9 \cdot 10^{-4}$ m. The membrane is laminated onto the fibers to enhance dust separation efficiency and enables lower dust penetration into the filter medium. This filter medium has a base weight of $290\,g/m^2$ and an air permeability (at 200 Pa) of $35\,L/dm^2min$. Both geometries, flat and pleated, were fabricated from the same filter medium, allowing a comparison of their operating behavior.

2.1.3. Implementation of pleated filter media into the test-rig

The implementation of both the flat and pleated filter media into the test rig is shown in Fig. 2. The flat filter medium coupon is implemented into the test-rig by using a circular metal filter holder with a flow cross-section of $0.015\,m^2$. The filter medium is placed into the holder and a support bar structure for more stability is added on the clean gas side behind the filter medium. If correctly dimensioned, the filter holder with the flat filter medium is self-sealing.

For the pleated filter medium, as shown in Fig. 2, a different technique is employed. A two-part 3D-printed structure (black) is used to secure the pleated filter medium with a defined pleat ratio. The filter medium is sealed into the structure using silicone. The two-part structure is then inserted into a circular metal filter holder and the gap between the structure and the metal filter holder is sealed by using a gasket. The flow cross-section of the pleated setup is $0.0081\,m^2$, which is smaller than that of the flat coupon, however, the filter surface area is larger due to pleating. The flat medium coupon has a surface area

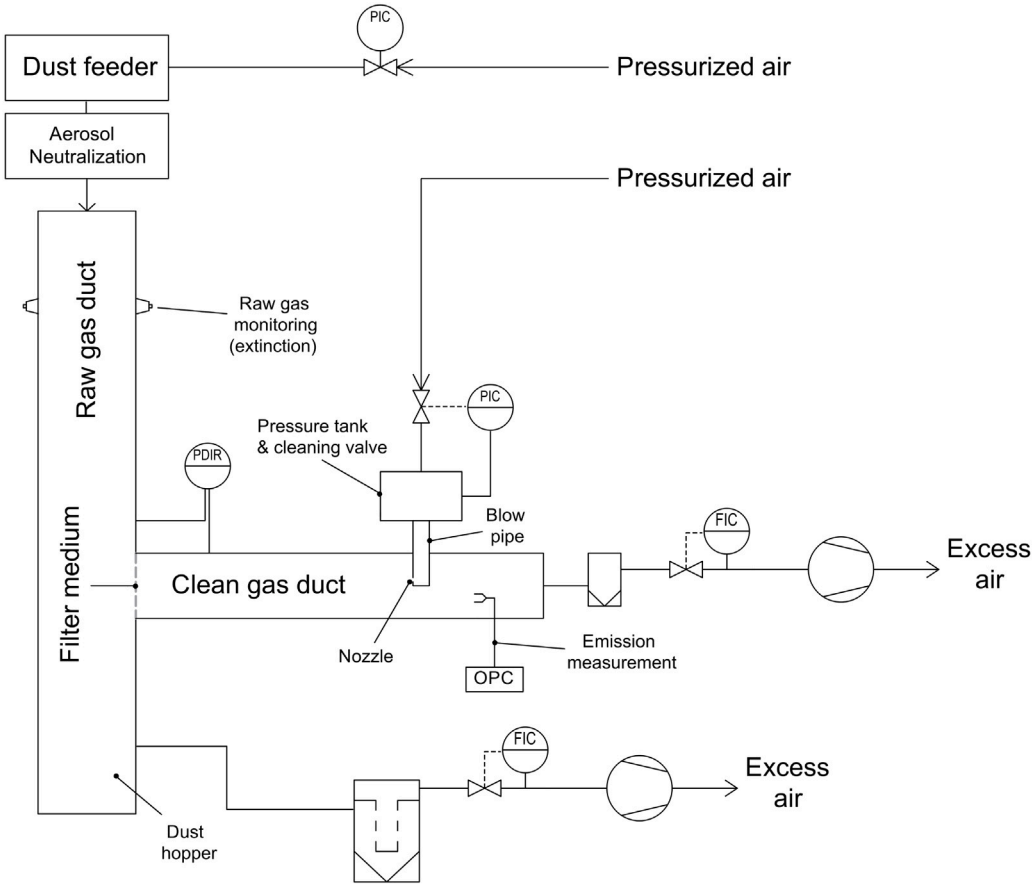

Fig. 1. Adapted schematic setup of the test-rig based on DIN ISO 11057.

of $A_{\text{Filter}} = 0.015\,\text{m}^2$, whereas the pleated filter medium with a pleat ratio of 2 has $A_{\text{Filter}} = 0.031\,\text{m}^2$. This difference is due to the effort to maximize the available medium surface area within the given test-rig dimensions for the pleated geometry. The pleated filter medium is implemented with a pleat ratio of 2, corresponding to a pleat height of $19 \cdot 10^{-3}\,\text{m}$ and a pleat pitch (tip to tip) of $9.5 \cdot 10^{-3}\,\text{m}$. Due to the different height of the filter elements the circular metal filter holder for the pleated geometry is $0.017\,\text{m}$ higher, compared to the holder for the flat geometry. This difference is necessary, to accommodate the pleat height within the two-part 3D-printed structure.

2.1.4. Adaptation of the pulse-jet intensity for both media geometries

Due to the use of different metal filter holders, an adaptation of the flange on the clean gas side is necessary for the pleated filter media holder. This modification altered the distance between the outlet of the blow pipe and the surface of the filter medium, if the side of the medium facing the raw gas duct is used as the reference point. To evaluate the effect of this distance change on regeneration intensity, the pulse-jet pressure was measured using a perforated calibration plate. This plate, as specified in DIN ISO 11057, is used to calibrate the pressure pulse of the regeneration unit. It matches the diameter of a flat filter coupon and is perforated in a circular pattern with eight perforations. A schematic of the perforated plate positioning relative to the blow pipe is shown in Fig. 3. The new flange for the pleated filter medium increased the distance to the blow pipe by $0.002\,\text{m}$ compared to the flat filter medium configuration. The height increase of the filter holder is implied by the green markings in Fig. 3. A schematic figure of the implementation for both medium geometries can be seen in the Appendix of this manuscript. The measurement of the maximum peak pressure was conducted directly on the surface of the perforated plate, as implied by the red dots in Fig. 3.

To evaluate regeneration intensity, the maximum peak pressure during pulse-jet regeneration was measured directly at the medium surface. The schematic position of the measurement at the filter medium surface can again be seen in Fig. 3. An exemplary pressure–time curve of a pulse-jet with the perforated plate is illustrated in Fig. 4. The maximum peak pressure is the maximum of the differential pressure curve. Another important factor is the duration of the peak. Due to the flow resistance of the perforated plate the baseline signal of the differential pressure is slightly negative. After the regeneration pulse is triggered the differential pressure signal increases and becomes positive. After a short time the signal decreases to reach the baseline signal again. In this study the duration of the regeneration peak was determined by the duration of the positive differential pressure signal. Both the duration of the regeneration and the height in differential pressure are critical indicators of regeneration intensities. A reduced maximum peak pressure typically correlates with less effective dust cake removal, especially for pleated media, where sufficient peak pressure is crucial for thorough regeneration [17,18,23].

Measurements were performed by inserting the perforated plate into each circular metal filter holder and setting the volumetric flow to $2.6 \cdot 10^{-4}\,\text{m}^3/\text{s}$. This flow rate corresponds to a filter medium face velocity of $w_{\text{Filter}} = 1\,\text{m}/\,\text{min}$ for the flat media coupon. The tank pressure was set to $0.5\,\text{MPa}$, the electric valve opened for $t_{\text{Valve}} = 60\,\text{ms}$. The regeneration pulses were manually triggered and the maximum peak pressure was recorded three times for each setup. The exemplary differential pressure curve in Fig. 4 shows that the maximum differential pressure exceeds the required minimal value for the maximum differential pressure set in DIN ISO 11057 [13] of $3200\,\text{Pa}$ and the duration of the regeneration peak is $700\,\text{ms}$. This means the required maximum peak pressure and the peak duration achieved are in accordance to DIN ISO 11057.

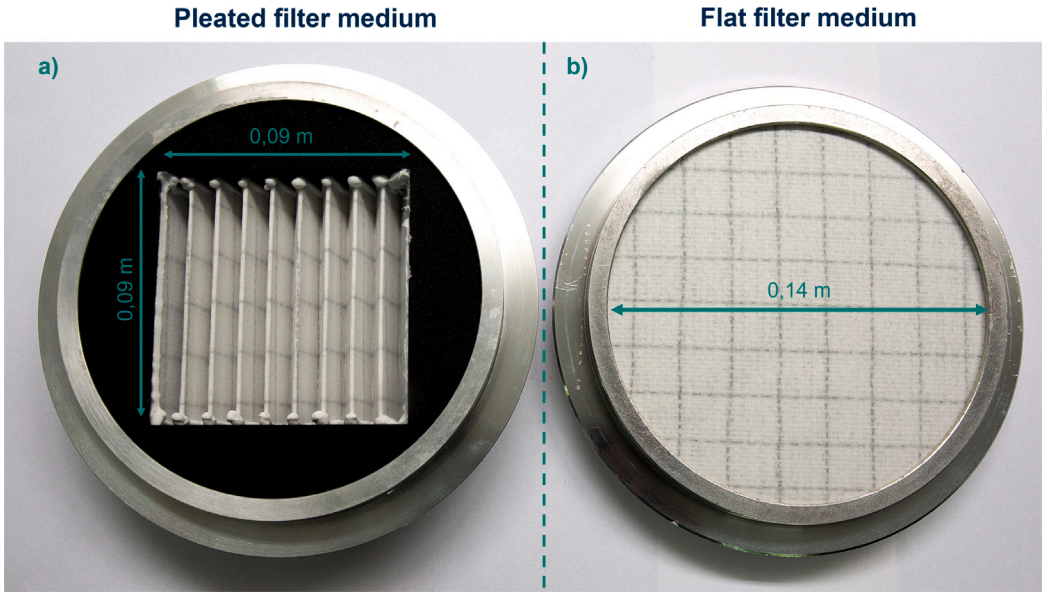

Fig. 2. Filter medium holder for the test-rig for a pleated filter medium (pleat ratio of 2) (a) and a flat medium coupon (b).

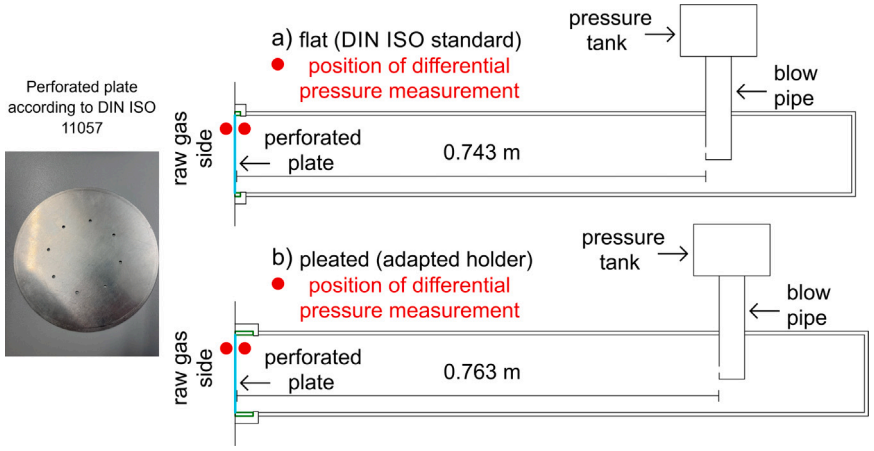

Fig. 3. Positioning and distance of the perforated plate in the test-rig for the adaptation of flat filter media (a) and for pleated filter media (b).

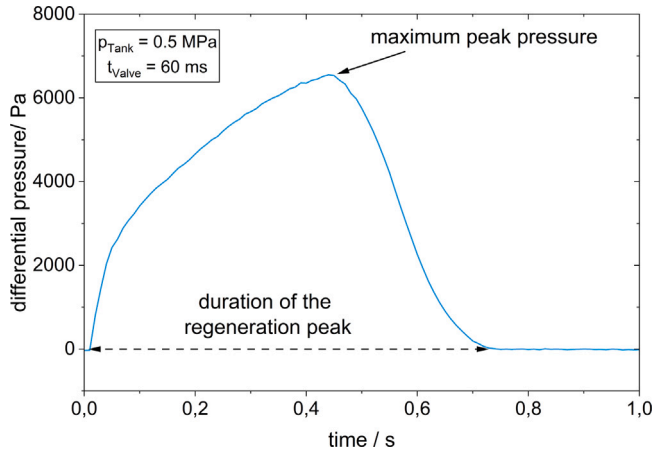

Fig. 4. Exemplary differential pressure curve of a regeneration pulse with the perforated plate for a blow pipe distance of 0.763 m.

The results for the different blow pipe distances are shown in Fig. 5. The dotted lines illustrate the mean value, as a result of triple determination, of the maximum peak pressure for each geometry. The mean maximum peak pressure for the flat geometry was 6183 Pa and 6085 Pa for the pleated configuration, resulting in a deviation of only 1.5%. This indicates that the increased blow pipe distance introduced by the new flange did not significantly affect the regeneration intensity. The differences in the start time of the differential pressure ramp after the regeneration was due to manually triggering the measurement. During highly time resolved measurements the delay due to manually triggering the pulse-jet leads to a slightly different beginning of the differential pressure curve, even while attempting to trigger the regenerations in the same time intervals.

For a valid comparison between the two media geometries, experimental conditions must be harmonized. Although the pleated medium has a smaller flow cross-section (0.0081 m^2 vs. 0.015 m^2), its total filter surface area is larger due to pleating. Therefore, the volumetric flow and dust dosage rate were adjusted proportional to the filter face area of the respective geometry to maintain a constant filter medium face velocity and raw gas concentration for both configurations.

However, regeneration intensities also had to be harmonized, which do not necessarily follow a simple proportionality with the filter face

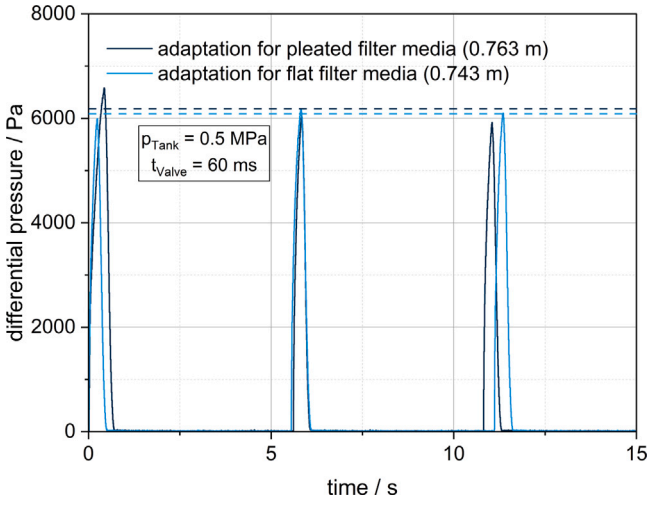

Fig. 5. Differential pressure curves of the regeneration for both adaptation flanges for the pleated and flat geometry.

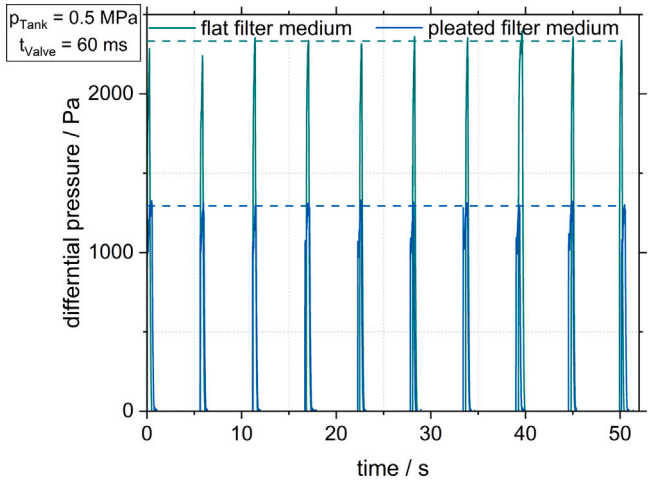

Fig. 6. Differential pressure curves of the regeneration the flat and pleated membrane filter medium.

area. Fig. 6 shows the differential pressure curves under identical regeneration conditions (p_{Tank} = 0.5 MPa, t_{Valve} = 60 ms). Due to the larger surface area of the pleated media, the maximum peak pressure is lower, leading to reduced cleaning efficiency. The differential pressure curves show, that the mean value for the maximum peak pressure (dotted lines) is higher for the flat filter medium. This is due to the increase in filter medium surface area for the pleated geometry. Conceptually, the pulse-jet can be interpreted as a volumetric flow counteracting the nominal flow direction; with a larger surface area, the face velocity of the jet is reduced, resulting in less intense regeneration for the pleated filter medium under the same regeneration parameters.

As the test-rig is limited to a maximum tank pressure of 0.5 MPa, the tank pressure for the flat filter medium was adjusted (more precisely, reduced) to enable the same maximum peak pressure for both geometries. Fig. 7 presents the mean maximum peak pressure as a function of tank pressure for the flat filter medium, showing a linear relationship. Each mean value represents the mean of the maximum peak pressure of 10 regenerations. Following the linear dependency of the maximum peak pressure and tank pressure, a tank pressure of 0.19 MPa is required for the flat medium to match the 1180 Pa maximum peak pressure of the pleated medium at 0.5 MPa. The results of the changed tank pressure for the flat geometry compared to the pleated are resembled by the red

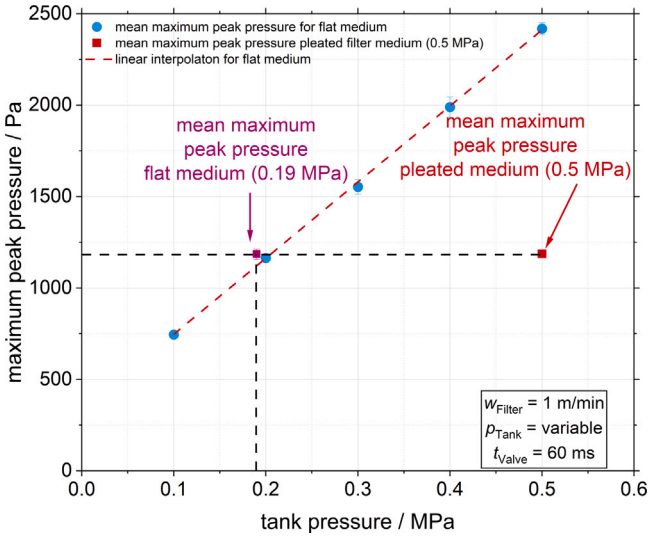

Fig. 7. Maximum peak pressure at different tank pressures for the flat filter medium.

and purple data point. Both points again represent the mean value of 10 maximum peak pressures for each medium geometry. The purple point is slightly offset from the intersection of the linear regression, as the calculated tank pressure of about 0.19–0.2 MPa was subsequently fine-tuned experimentally to achieve equal regeneration intensity for the flat and pleated media. This showing, that the adjustment of the tank pressure for the flat medium geometry to 0.19 MPa enables the same maximum peak pressure for the flat and pleated filter medium.

Pulse durations for both geometries varied between 600–800 ms, independent of the respective geometry. The observed variations are caused by electrical latencies within the communication system of the regeneration unit and by the difference between the electrical signal delay and the mechanical response time of the valve. The delays between electric and mechanical opening time can lead to a longer release of pressurized air during regeneration. Nevertheless, the peak pulse duration is still in accordance with DIN ISO 11057.

Ultimately, comparable and reliable characterization of the filter media geometries is only possible when the parameters filter medium face velocity, dust loading, and regeneration intensity are consistently aligned.

2.2. Experimental methodology

To characterize and compare the different filter media geometries, the experimental procedure outlined in the DIN ISO 11057 guideline was adapted. A comparison of the experimental procedures is shown in Fig. 8.

The experimental procedure for characterization of cleanable filter media consists of three phases. In the first phase (conditioning) Δp-controlled cycles are conducted to assess the behavior of a factory-new filter medium. The conditioning cycles in this study were reduced from 30 to three. The Δp-controlled cycles were conducted with a maximum allowed differential pressure of 500 Pa. After exceeding the maximum allowed differential pressure regeneration was triggered. The allowed maximum differential pressure is reduced to enable comparable dust cake thicknesses under adjusted operating conditions (see Section 2.3). The reduction of the conditioning cycles, which are used to evaluate the operating behavior of new filter media, was done to reduce the duration of the experiments, as the focus of this study was primarily on the aged stage of the filter media. The second phase (artificial aging) is needed to simulate long term use of the filter medium. The artificial aging stage in this study consisted of 500 Δt-controlled cycles with a

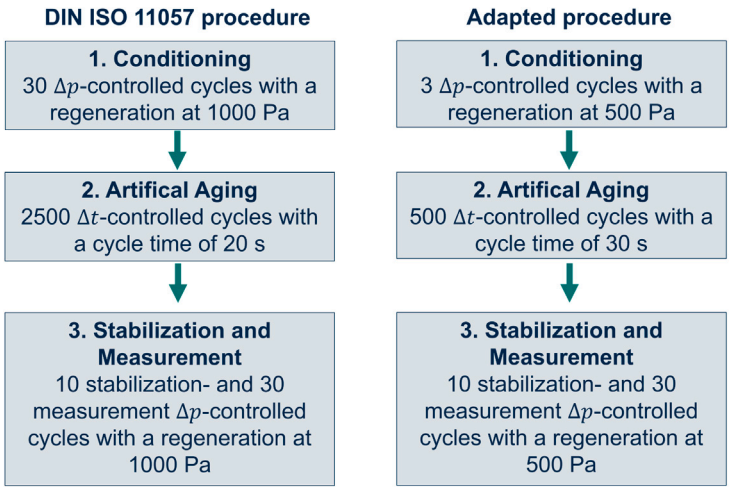

Fig. 8. DIN ISO 10057 and adapted experimental procedure for characterization of filter media.

cycle duration of 30 s, resulting in a regeneration of the filter medium every 30 s. The cycle time was selected based on previous experiments in the same test-rig, which demonstrated that this time sufficiently ages filter media with respect to residual differential pressure and particle emissions [24]. The reduction in aging cycles was based on the sufficient aging of the filter medium after 500 cycles, as shown in Section 3.2. Following the artificial aging phase 10 stabilizing (required to stabilize experimental parameters after aging) and 30 measurement cycles (Δp-controlled) with a regeneration at a differential pressure of 500 Pa were conducted. These cycles are essential to characterize and evaluate the operating behavior. The procedure was performed for the flat and pleated geometry (pleat ratio 2) of the same filter media. Key parameters for the evaluation of the operating behavior were the cycle time and the residual differential pressure.

2.3. Experimental parameters

The experimental parameters influencing the operating behavior of surface filters are characterized in DIN ISO 11057 and have been adapted to fit the experiments conducted in this study. The experimental parameters are listed comparatively in Table 1. The deviation of the parameters set by the ISO-norm has several reasons. The filter medium surface area varies between the flat and pleated geometry, as explained in Section 2.1.3. This meaning, the tank pressure has to be adapted for the flat filter medium to ensure the same intensity of regeneration, represented by the maximum peak pressure. The detailed explanation of the adaptation of p_{Tank} is given in Section 2.1.4.

The filter medium face velocity in this study was adjusted to $w_{\mathrm{Filter}} = 1\,\mathrm{m/min}$, to reproduce typical operating conditions for pleated or pleatable filter media and elements according to VDI 3766 [25]. Due to the, compared to DIN ISO 11057, lower w_{Filter} in this study the raw gas concentration c_{Raw} and the maximum differential pressure before regeneration Δp_{Max} had to be changed. These changes are necessary to ensure the same amount of dust per time unit to reach the surface of the filter medium as in the ISO-norm, as well as a comparable cake height at the end of each filtration cycle. Furthermore, the cycle time ($\Delta t_{\mathrm{Cycle}}$) for the artificial aging phase in this study was increased to 30 s. This was done due to previous studies conducted in the same test-rig, that sufficiently aged filter media with a $\Delta t_{\mathrm{Cycle}} = 30\,\mathrm{s}$ [24].

As mentioned before, the experimental parameters were adapted for both geometries to ensure the same experimental conditions. The filter medium face velocity was set to $w_{\mathrm{Filter}} = 1\,\mathrm{m/min}$ and the raw gas concentration was set to $c_{\mathrm{Raw}} = 10\,\mathrm{g/m^3}$. Due to the increased surface area of the pleated filter medium compared to the flat coupon, both the volumetric flow and dust dosage rate were adjusted to maintain consistent filter medium face velocity and raw gas concentration across both geometries. The maximum differential pressure before regeneration was $\Delta p_{\mathrm{Max}} = 500\,\mathrm{Pa}$ during the conditioning, stabilizing and measurement phase. After exceeding the maximum differential pressure the electromagnetic valve of the regeneration unit was opened for 60 ms (electric pulse time). The pressure in the pressure tank was set to 0.5 MPa for the pleated geometry. The tank pressure for the flat medium coupon was set to 0.19 MPa, as outlined in Section 2.1.4. During the aging phase the filter medium face velocity, the raw gas concentration and the regeneration parameters remained unchanged. However, a Δt-controlled regeneration was triggered every 30 s ($\Delta t_{\mathrm{Cycle}} = 30\,\mathrm{s}$) for 500 cycles.

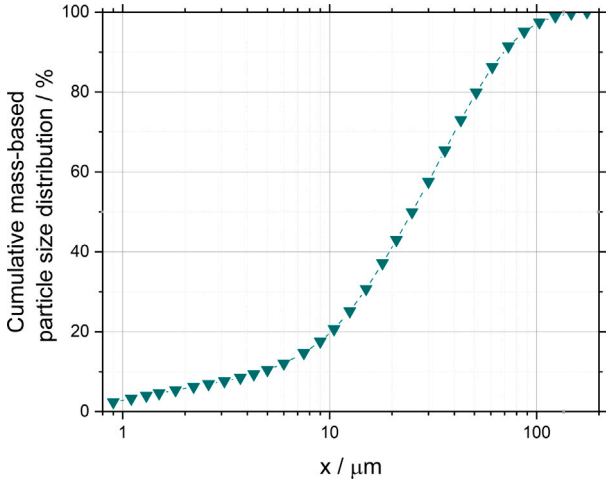

Fig. 9. Cumulative mass-based particle size distribution of PURAL®SB measured with Sympatec Helos & Rodos dry disperser.

2.4. Test dust

The test dust used was the relatively coarse Boehmite (AlO(OH)) PURAL®SB by Sasol with a $x_{50,3} = 25\,\mu\mathrm{m}$. The cumulative mass-based particle size distribution, measured using laser light ensamlbe scattering (Sympatec Helos & Rodos dry disperser), is in shown in Fig. 9.

The dust is non-agglomerating and free-flowing, making it easy to dose and benefits regeneration due to an easy removal of the dust cake. Previous studies [24,26] using the same test dust have shown,

Table 1
Comparison of the experimental parameters in DIN ISO 11057 and in this work.

	A_{Filter}/ m^2	w_{Filter}/ m/min	c_{Raw}/ g/m^3	Δp_{Max}/ Pa	p_{Tank}/ MPa	t_{Valve}/ ms	t_{Cycle}/ s
DIN ISO 11057	0.015	2	5	1000	0.5	60	20
flat filter medium	0.015	1	10	500	0.19	60	30
pleated filter medium	0.031	1	10	500	0.5	60	30

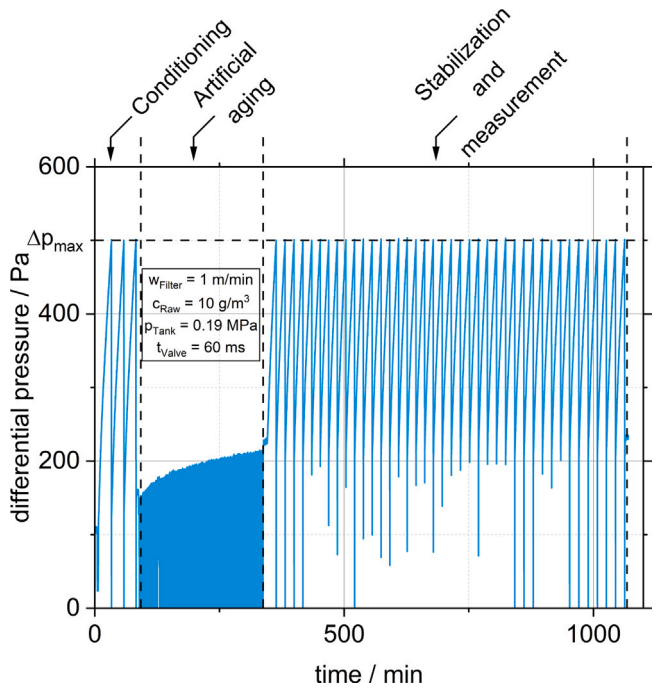

Fig. 10. Differential pressure curve depicting the three stages of the experimental methodology (conditioning, artificial aging, stabilization and measurement)

that it leads to detectable emission events on the clean gas side after regeneration, despite its low fine-dust fraction. This indicates that a sufficient number of particles in the size range of the most penetrating particle size (MPPS) for surface filters are present and capable of penetrating the filter medium.

3. Results and discussion

To characterize the impact of different filter medium geometries on the operating behavior the methodology described in Section 2.2 was applied. An exemplary differential pressure curve of a flat medium coupon over the course of the entire experiment is illustrated in Fig. 10. The dotted line marks the maximum allowed differential pressure for the conditioning, stabilization and measurement phase. When this threshold is exceeded, the regeneration is triggered, causing a decrease of the differential pressure due to dust cake removal.

The three phases of the experimental procedure are clearly identifiable. The experiment begins with the conditioning phase consisting of three Δp-controlled cycles. Once the maximum pressure drop is exceeded three times, the artificial aging begins. During this phase the Δt-controlled cycles lead to an gradual increase in the residual, as well as the maximum differential pressure over time. This is mainly due to particle deposition inside the filter medium during the aging. Following the aging phase, 10 cycles for stabilization and 30 measurement cycles were conducted, both showing the characteristic saw-tooth pattern for surface filters.

To characterize both media geometries, the cycle time and the residual differential pressure in the stabilization and measurement phase were evaluated. Here, the residual differential pressure being the differential pressure 12 s after regeneration and the cycle time corresponding to the duration between regenerations. This allows the evaluation of the influence of the different filter medium geometries on the operating behavior. These two parameters provide insight into the filtration performance and operational stability of each configuration. In particular, an unstable operating behavior would manifest with a rising residual differential pressure and a decreasing cycle time over successive cycles. To minimize the impact of measurement errors or batch-to-batch variation in filter medium properties, each geometry was tested three times.

3.1. Conditioning of both filter medium geometries

The purpose of the conditioning phase is to gain insight on the operating behavior of a new, unused filter media. The mean values for the cycle time and residual differential pressure of the three experiments for each geometry and their standard deviation as error bars are depicted in Fig. 11. Furthermore the initial differential pressure for both geometries is shown at the filtration cycle zero in the right graph.

A comparison of the cycle time of both geometries during the conditioning phase shows that the cycle time decreases for each filtration cycle. This can be attributed to an increase in the residual differential pressure due to dust deposition inside the filter medium. This effect is common for new, unused filter media [14] and results in a smaller usable span of the differential pressure before regeneration. The mean cycle time for the pleated filter medium is shorter than for the flat filter medium, but the differences in cycle time between both geometries are within the range of the error bars.

Considering the residual differential pressure and the initial differential pressure for both medium geometries a difference can be seen. The initial differential pressure for the new filter medium is about the same for both geometries. The initial differential pressure varies by 4% between the two geometries, showing that the change in geometry barely effects the initial differential pressure. The development of the residual differential pressure for the first three filtration cycles shows a lower residual differential pressure for the pleated geometry, even though the experimental parameters were adapted for both geometries. One would assume, that due to the pleating of the filter media a higher residual differential pressure would occur for the pleated geometry because of more difficult media cleaning and the remainder of dust inside the pleats. As this is not the case, a different deposition of particles inside the filter medium in the first cycles for the different geometries could result in a higher residual differential pressure. Furthermore, the increase in differential pressure during the conditioning phase differs for both geometries. The differential pressure increases 26 Pa for the flat and 11 Pa for the pleated geometry. These phenomena underlines the necessity to directly characterize pleated filter media, because a change in operating behavior or potential filter medium characteristics can already be seen during the first phase of testing the new filter media.

3.2. Artificial aging of both filter medium geometries

As mentioned in Section 2.2 the procedure from DIN ISO 11057 was adapted by reducing the number of aging cycles for both geometries to 500. To evaluate whether both medium geometries are sufficiently

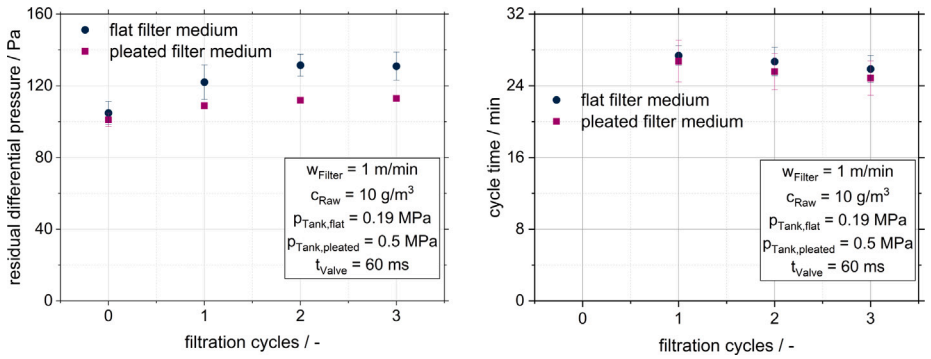

Fig. 11. Cycle time (left) and residual differential pressure (right) for the conditioning phase for both filter medium geometries.

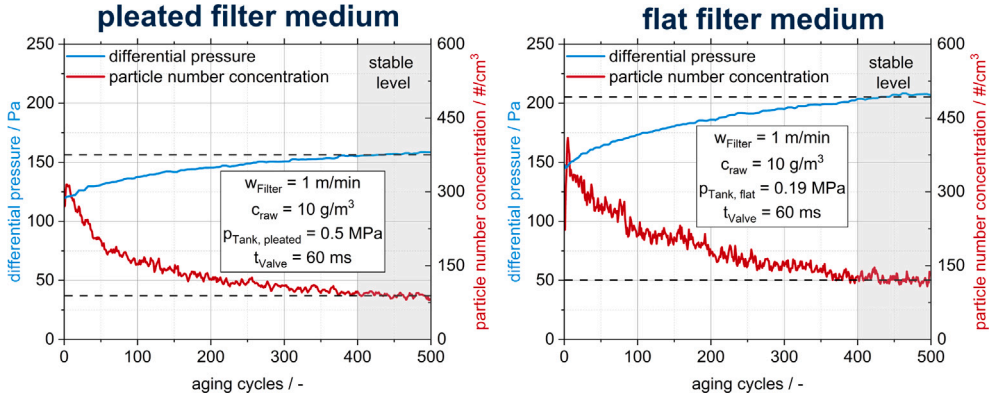

Fig. 12. Differential pressure and particle number concentration (30 s averaged values) in the detectable size range of the used sensor (0.2 – 10 μm) for both filter medium geometries during artificial aging.

aged, the development of the particle number concentration and differential pressure during aging must be considered. The goal is to reach stable levels of differential pressure and particle number concentration. In this study, a stable level is defined as the point at which both the differential pressure and the particle number concentration fluctuate around a near-constant value.

For the differential pressure, which increases with the aging cycles and appears to approach a constant level after approximately 400 cycles, the maximum value within each 30 s averaging interval was evaluated to account for the periodic signal fluctuations caused by the measurement process. The maximum value corresponds with the differential pressure immediately before each regeneration during the aging phase. A stable level was defined based on convergence towards the mean value of a predefined stable segment at the end of the measurement, more specific the last 400 cycles. The mean value and the corresponding standard deviation σ_{stable} was calculated for this segment. A data point was considered to be in steady state if its deviation from the mean value of the stable segment remained within a confidence band of $1.5 \cdot \sigma_{stable}$. A stable level was assumed to be reached once this condition was fulfilled for 50 consecutive cycles, corresponding to a duration of 25 min.

For the particle number concentration, which decreases over time and approaches a constant value after approximately 400 cycles, the minimum values within each 30 s averaging interval were analyzed to compensate for fluctuations introduced by the measurement equipment. The steady state was determined using the same convergence criterion and persistence requirement as described above.

The development of an exemplary aging stage for the pleated and flat filter medium is shown in Fig. 12. The constant value at the stable phase is schematically depicted by the black dotted lines. Both filter geometries show similar qualitative trends for the differential pressure and the particle number concentration. The particle number concentration for the flat and pleated filter medium decreases progressively over the cycles, stabilizing after about 400 cycles. Likewise, the differential pressure also stabilizes after 400 cycles, resulting in a sufficient aging for both filter geometries. The decrease in particle number concentration and the increase in differential pressure can be attributed to an increase of particles deposited inside the filter medium. The deposition is beneficial for particle separation, as fewer particles penetrate through the filter medium. As a result the flow resistance of the medium is increased, leading to an increase in differential pressure.

As shown in Fig. 12, a difference between the aging behavior of the two medium geometries for the same filter medium can be seen. The pleated geometry starts the aging phase with an emission level of 335 particles per cm^3 after the first cycles, compared to the flat filter medium which starts at about 410 particles per cm^3. The increase of particle number concentration after the first few cycles is the result of the execution of the experiment, as the dust dosing is started manually, resulting in a certain start-up effect until the actual emission level is reached. The factor of the decrease of the particle number concentration from start to end value after the 500th cycle however is four for both geometries. The rise in differential pressure also differs for both geometries. Due to a different development of the rise in residual differential pressure, depicted in Fig. 11, the flat filter medium starts the aging phase with a differential pressure of 147 Pa, whereas the pleated medium depicts a differential pressure of 119 Pa. During the aging phase the continuous deposition of particles inside the filter medium leads to an increase of differential pressure of 59 Pa for the flat and 40 Pa for the pleated filter medium. This resulting in a higher differential pressure after filter medium aging for the flat geometry (206 Pa), compared to the pleated geometry (159 Pa) and consequently leading to a lower usable differential pressure span for filtration in the stabilization and measurement phase for the flat filter medium.

The curves in Fig. 12 exemplarily show the aging for one pleated and one flat filter medium. The other two experiments for each geometry show the same qualitative trend for both the development of differential pressure and particle number concentration, but are omitted to avoid repetition.

3.3. Evaluation of the operating behavior of the flat and pleated filter medium during the measurement phase

The final experimental phase consists of 10 stabilizing and 30 measurement cycles. The cycles are Δp-controlled with a regeneration at a differential pressure of 500 Pa. To characterize both filter medium geometries the residual differential pressure and the cycle time were considered. Fig. 13 shows the development of the residual differential pressure for the flat and pleated filter medium. The residual differential pressure is shown for the conditioning stage (phase 1), as well as the stabilization and measurement stages (phase 3). The aging phase is not shown for reasons of clarity. The aging of the filter media is indicated by the arrows after the three conditioning cycles. More information concerning the artificial aging can be seen in Section 3.2 The initial differential pressure for both geometries (105 Pa for the flat and 101 Pa for the pleated medium) differ slightly. The difference in the initial differential pressure can partially be attributed to a change in medium resistance due to the pleating process and the mechanical stress applied to the filter medium or the partial destruction of the membrane during pleating. Both filter medium geometries show a similar trend: a slight increase in residual differential pressure during the conditioning stage, with a higher increase of 26 Pa for the flat geometry. During aging the differential pressure increased about 56 Pa for the flat and 46 Pa for the pleated filter medium, respectively. As a result of its higher initial differential pressure and a larger increase during conditioning and aging, the flat filter medium exhibited a higher overall residual differential pressure of 185 Pa during stabilization and measurement, compared to 165 Pa of the pleated geometry. The higher residual differential pressure is the result of a different behavior of the flat filter medium during conditioning and aging, compared to the pleated filter medium. The change in media geometry and the resulting potential change in filter medium characteristics can result in a different particle deposition inside the filter media during the first cycles and the aging phase, affecting the residual differential pressure.

The stabilization and measurement phase begins after the artificial aging stage. Both medium geometries demonstrate a stable residual differential pressure development after aging, where no steady increase of residual differential pressure over the course of the stabilization and measurement stage was noted. An increase in the residual differential pressure over time would be an indicator for unstable filter operation. The stable operation furthermore shows, that the reduced number of aging cycles sufficiently age both medium geometries. Despite identical experimental conditions, the pleated medium consistently showed a 12% lower residual differential pressure compared to the flat geometry.

In addition to the residual differential pressure, the development of the cycle time provides further insights into stable filter operation of both geometries. Fig. 14 illustrates the trend of the cycle time for both configurations. Again 43 cycles are shown, three from conditioning, 10 from stabilization and 30 from measurement. The aging cycles are omitted for clarity.

The pleated medium exhibits an averaged cycle time across all stabilization and measurement cycles of 21 min, while the flat medium shows a shorter averaged cycle time of 19 min. The difference in cycle time can partly be attributed to the difference in residual differential pressure. The higher residual differential pressure of the flat medium reduces the differential pressure range for cake build-up until the allowed maximum differential pressure is exceeded. This effect leads to shorter cycle times, as observed for the flat filter medium. However, a lower residual differential pressure does not directly correlate to a complete dust cake removal from filter medium due to regeneration.

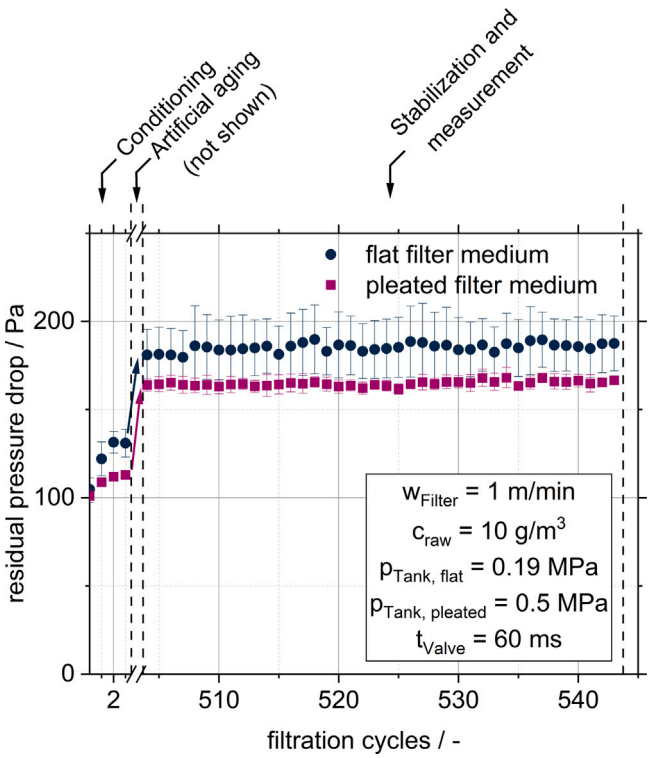

Fig. 13. Development of the residual differential pressure for the flat and pleated filter medium.

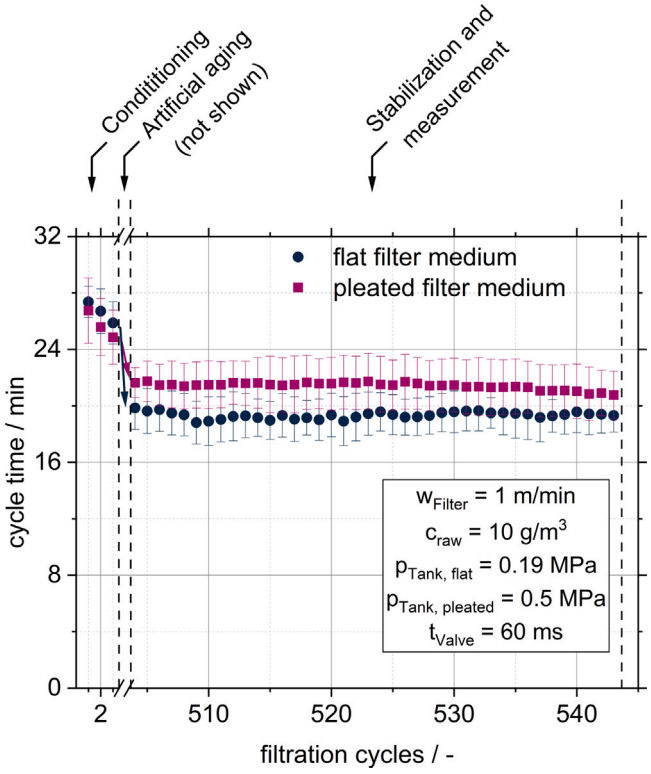

Fig. 14. Development of the cycle time for the flat and pleated filter medium.

The residual differential pressure can be low, but effects such as patchy-cleaning and dust cake compression can lead to an increasing rate of differential pressure rise [14].

When comparing the slopes of the differential pressure increase in the first 60 s after regeneration and the last 60 s before the regeneration, a further difference between the filter media geometry becomes evident. The flat filter medium has an average slope of 33 Pa/min directly after regeneration and 16 Pa/min at the end of each cycle, indicating a steep initial increase followed by a slower rise of the differential pressure during cake filtration. The differential pressure of the pleated filter medium exhibits slopes of 26 Pa/min immediately after regeneration and 17 Pa/min at the end of each cycle, resulting in a more linear increase of differential pressure over time. The different slopes and the different residual differential pressure result in a 10% shorter cycle time for the flat geometry during the measurement phase, as the maximum allowed differential pressure is reached sooner.

These findings contrast with the general consensus that pleated filter elements show less effective regeneration, typically resulting in higher residual pressure drops, different slopes of the differential pressure during dust loading and shorter cycle times [10,16,17]. As most studies evaluate the first filtration cycles of unused, not aged, filter media and do not harmonize the experimental parameters the change in cycle time can only be partly contributed to the pleated geometry. The same experimental procedure and parameters for both media geometries, enable the allocation of differences in operating behavior based on the filter medium geometry. It shows that under certain experimental circumstances (e.g. using a free flowing, coarse dust and evaluating the specific medium geometries of a membrane filter medium) the influence of media geometry can lead to a deviation of the general assumption, as in this study the cycle time for the pleated filter medium was higher, compared to the flat medium geometry.

4. Conclusion and outlook

This study investigated the influence of filter medium geometry on the operating behavior of cleanable surface filters by directly comparing a flat filter medium coupon with its pleated counterpart under harmonized experimental conditions. An adapted DIN ISO 11057 procedure, combined with a novel filter holder for the pleated medium geometry, enabled geometry-dependent effects to be isolated under identical operating conditions.

The results demonstrate that the operating behavior of pleated filter media cannot be reliably inferred from flat coupon tests alone. Under identical conditions, the pleated filter medium exhibited a lower residual differential pressure after aging and stabilization, corresponding to a reduction of approximately 12 %, and a longer cycle time during the measurement phase, increasing by about 10 % compared to the flat medium. Analysis of the differential pressure evolution and slope within individual filtration cycles further revealed geometry-dependent differences in dust cake formation. The flat filter medium showed a pronounced initial increase in differential pressure immediately after regeneration, whereas the pleated medium exhibited a more linear pressure increase over time. As a result, the maximum allowable differential pressure was reached earlier for the flat filter medium, leading to shorter cycle times.

These findings contrast with the commonly reported assumption that pleated filter elements generally exhibit less effective regeneration of the filter medium and shorter cycle times compared to flat media. The present results indicate that, when experimental parameters are harmonized and aged filter media are considered, pleated filter media can exhibit comparable or improved operating behavior, particularly under conditions involving free-flowing, coarse dust, which benefits dust cake removal. This highlights that geometry alone cannot explain previously reported differences, which are strongly influenced by test conditions, aging state of the filter media, and regeneration intensity.

The presented methodology provides a reproducible methodology for the direct characterization of pleated filter media in pulse-jet-cleaned test rigs. It enables systematic investigation of geometric effects independent of experimental parameters and supports improved interpretation of filtration behavior of pleated filter media. Future work should extend this approach to different pleat ratios, pleat geometries, and dust types to further clarify the role of geometry in filter performance and to support the development of more reliable testing methodologies for pleated filter media.

CRediT authorship contribution statement

Jakob Paul Knisley: Writing – review & editing, Writing – original draft, Visualization, Validation, Project administration, Methodology, Investigation, Data curation, Conceptualization. **Jörg Meyer:** Writing – review & editing, Formal analysis, Conceptualization. **Achim Dittler:** Writing – review & editing, Supervision, Resources, Funding acquisition, Conceptualization.

Declaration of Generative AI and AI-assisted technologies in the writing process

During the preparation of this manuscript, the authors used ChatGPT 5 (OpenAI) to improve language clarity and readability. All scientific content, interpretations and conclusions were produced and verified by the authors. The authors take full responsibility for the accuracy and integrity of the work.

Declaration of competing interest

The authors declare that they have no known competing financial interests or personal relationships that could have appeared to influence the work reported in this paper.

Acknowledgments

We acknowledge the financial support and the close cooperation of the Filterkonsortium at KIT. The Filterkonsortium at KIT unites leading companies in the fields of fiber and media production, assembly, plant engineering and measurement technology with the research activities of the research group Gas-Particle-Systems of the Institute of Mechanical Process Engineering and Mechanics (MVM). The members of Filterkonsortium at KIT are as follows: BWF Tec GmbH & Co. KG, BWF Envirotec, ESTA Apparatebau GmbH & Co. KG, Freudenberg Filtration Technologies GmbH & Co. KG, Junker-Filter GmbH, MANN+HUMMEL GmbH, and Palas GmbH.

Appendix A. Supplementary data

Supplementary material related to this article can be found online at https://doi.org/10.1016/j.seppur.2025.136720.

Data availability

Data will be made available on request.

References

[1] F. Löffler, Staubabscheiden, Lehrbuchreihe Chemieingenieurwesen / Verfahrenstechnik, Georg Thieme, Stuttgart, 1988.
[2] D. Leith, M.J. Ellenbecker, Dust emission characteristics of pulse-jet-cleaned fabric filters, Aerosol Sci. Technol. 1 (4) (1982) 401–408, http://dx.doi.org/10.1080/02786828208958604.
[3] E. Bakke, Optimizing filtration parameters, J. Air Pollut. Control Assoc. 24 (12) (1974) 1150–1154, http://dx.doi.org/10.1080/00022470.1974.10470027.
[4] E. Schmidt, Abscheidung von Partikeln aus Gasen mit Oberflächenfiltern, in: Fortschritt-Berichte VDI, no. 3, VDI Verlag GmbH, Düsseldorf, 1998.
[5] T. Dziubak, L. Bąkała, S.D. Dziubak, K. Sybilski, M. Tomaszewski, Experimental research of fibrous materials for two-stage filtration of the intake air of internal combustion engines, Materials 14 (23) (2021) 7149, http://dx.doi.org/10.3390/ma14237166.

[6] W. Hoeflinger, T. Laminger, Standard test procedure to characterise different filter media under energy consideration, Energy Sustain. 176 (4) (2013) 145–155, http://dx.doi.org/10.2495/ESUS130121.
[7] J. Binnig, J. Meyer, G. Kasper, Origin and mechanisms of dust emission from pulse-jet cleaned filter media, Powder Technol. 189 (1) (2009) 108–114, http://dx.doi.org/10.1016/j.powtec.2008.06.012.
[8] P. Bächler, J. Meyer, A. Dittler, Operating behavior of pulse jet-cleaned filters regarding energy demand and particle emissions – Part 1: Experimental parameter study, Chem. Eng. Technol. 46 (8) (2023) 1689–1697, http://dx.doi.org/10.1002/ceat.202300080.
[9] L.-M. Lo, D.-R. Chen, D.Y. Pui, Experimental study of pleated fabric cartridges in a pulse-jet cleaned dust collector, Powder Technol. 197 (3) (2010) 141–149, http://dx.doi.org/10.1016/j.powtec.2009.09.007.
[10] G. Teng, G. Shi, J. Zhu, J. Qi, C. Zhao, Research on the influence of pleat structure on effective filtration area during dust loading, Powder Technol. 395 (2022) 207–217, http://dx.doi.org/10.1016/j.powtec.2021.09.062.
[11] B.H. Park, M.-H. Lee, Y.M. Jo, S.B. Kim, Influence of pleat geometry on filter cleaning in PTFE/glass composite filter, J. Air Waste Manage. Assoc. 62 (11) (2012) 1257–1263, http://dx.doi.org/10.1080/10962247.2012.696530.
[12] S. Li, S. Hu, B. Xie, H. Jin, J. Xin, F. Wang, F. Zhou, Influence of pleat geometry on the filtration and cleaning characteristics of filter media, Sep. Purif. Technol. 210 (2019) 38–47, http://dx.doi.org/10.1016/j.seppur.2018.05.002.
[13] DIN ISO 11057: Air quality – Test method for filtration characterization of cleanable filter media (ISO 11057:2011), Standard, Berlin, Beuth Verlag GmbH, 2012.
[14] VDI 3926 – Part 1: Testing of cleanable filter media – Standard test for the evaluation of cleanable filter media, Guideline, Berlin, Beuth Verlag GmbH, 2004.
[15] S. Kang, N. Bock, J. Swanson, D.Y. Pui, Characterization of pleated filter media using particle image velocimetry, Sep. Purif. Technol. 237 (2020) 116333, http://dx.doi.org/10.1016/j.seppur.2019.116333.
[16] J.S. Kim, M.-H. Lee, Measurement of effective filtration area of pleated bag filter for pulse-jet cleaning, Powder Technol. 343 (2019) 662–670, http://dx.doi.org/10.1016/j.powtec.2018.11.080.
[17] Q. Zhang, D. Liu, M. Wang, Y. Shu, H. Xu, H. Chen, Characteristics and evaluation index of pulse-jet dust cleaning of filter cartridge, Process. Saf. Environ. Prot. 157 (2022) 362–374, http://dx.doi.org/10.1016/j.psep.2021.11.028.
[18] Q. Li, M. Zhang, Y. Qian, F. Geng, J. Song, H. Chen, The relationship between peak pressure and residual dust of a pulse-jet cartridge filter, Powder Technol. 283 (2015) 302–307, http://dx.doi.org/10.1016/j.powtec.2015.05.038.
[19] J. Li, S. Li, F. Zhou, Effect of cone installation in a pleated filter cartridge during pulse-jet cleaning, Powder Technol. 284 (2015) 245–252, http://dx.doi.org/10.1016/j.powtec.2015.06.071.
[20] C. Yan, G. Liu, H. Chen, Effect of induced airflow on the surface static pressure of pleated fabric filter cartridges during pulse jet cleaning, Powder Technol. 249 (2013) 424–430, http://dx.doi.org/10.1016/j.powtec.2013.09.017.
[21] J.-U. Kim, J. Hwang, H.-J. Choi, M.-H. Lee, Effective filtration area of a pleated filter bag in a pulse-jet bag house, Powder Technol. 311 (2017) 522–527, http://dx.doi.org/10.1016/j.powtec.2017.02.013.
[22] G. Teng, G. Shi, J. Zhu, Influence of pleated geometry on the pressure drop of filters during dust loading process: Experimental and modelling study, Sci. Rep. 12 (1) (2022) 20331, http://dx.doi.org/10.1038/s41598-022-24838-7.
[23] J. Sievert, F. Löffler, Fabric cleaning in pulse-jet filters, Chem. Eng. Process.: Process. Intensif. 26 (2) (1989) 179–183, http://dx.doi.org/10.1016/0255-2701(89)90010-X.
[24] P. Bächler, J. Meyer, A. Dittler, Characterization of the emission behavior of pulse-jet cleaned filters using a low-cost particulate matter sensor, Gefahrstoffe 79 (11–12) (2019) 443–450.
[25] VDI 3677 – Part 1: Filtering separators – Surface filters, Guideline, Berlin, Beuth Verlag GmbH, 2023.
[26] O. Kurtz, J. Meyer, G. Kasper, Influence of filter operating parameters on fine dust emissions from pulse-cleaned filter bags, Chem. Eng. Technol. 39 (3) (2016) 435–443, http://dx.doi.org/10.1002/ceat.201500340.